



HAL
open science

Piezoelectric actuation mechanisms for intelligent sandwich structures

Ayech Benjeddou, Marcelo Areias Trindade, Roger Ohayon

► **To cite this version:**

Ayech Benjeddou, Marcelo Areias Trindade, Roger Ohayon. Piezoelectric actuation mechanisms for intelligent sandwich structures. *Smart Materials and Structures*, 2000, 9 (3), pp.328-335. 10.1088/0964-1726/9/3/313 . hal-03179643

HAL Id: hal-03179643

<https://hal.science/hal-03179643>

Submitted on 15 Sep 2023

HAL is a multi-disciplinary open access archive for the deposit and dissemination of scientific research documents, whether they are published or not. The documents may come from teaching and research institutions in France or abroad, or from public or private research centers.

L'archive ouverte pluridisciplinaire **HAL**, est destinée au dépôt et à la diffusion de documents scientifiques de niveau recherche, publiés ou non, émanant des établissements d'enseignement et de recherche français ou étrangers, des laboratoires publics ou privés.

Piezoelectric actuation mechanisms for intelligent sandwich structures

A Benjeddou, M A Trindade and R Ohayon

Structural Mechanics and Coupled Systems Laboratory,
Conservatoire National des Arts et Métiers, 2, rue Conté, 75003, Paris, France

Abstract. Surface-mounted piezoelectric materials poled in the same direction as the applied electric field are known to induce membrane strains only. This could be seen as their conventional *extension actuation mechanism*. However, when piezoelectric materials are constrained and poled perpendicularly to the applied electric field, they act through their shear modes. This is the newly defined *shear actuation mechanism*. The present paper compares both mechanisms with the help of an adaptive sandwich beam finite element, with either active surface layers (for the extension mechanism) or active core (for the shear mechanism). Segmented configurations are studied for cantilever beams. Deflection, stress and vibration characteristics are compared for various parameters (structure/actuator stiffness and thickness ratios, actuator position and length). The shear actuation mechanism is found to present several promising features for brittle piezoceramics' use. In particular, it was found that the *shear actuation mechanism* is more efficient than the *extension* mechanism for stiff structures and thick piezoelectric actuators.

1. Introduction

Piezoelectric materials used to control noise and vibration, either surface-mounted or embedded in host structures, are commonly poled parallel to the applied electric field. Hence, they act through their conventional extension mechanism. This was extensively used and studied in the literature either in purely active [8, 9] or hybrid passive-active systems [1, 10, 17, 20]. A review of recent advances in modeling and applications of piezoelectric materials in active and hybrid active-passive vibration control of flexible structures can also be found in [3, 7, 16]. Using interdigitated electrodes (IDE), transverse actuation, through e_{33} or d_{33} piezoelectric constant can also be introduced [9]. However, constrained piezoelectric materials, poled perpendicular to the imposed electric field, use their thickness shear mode, leading to the less known shear actuators. Although mentioned by Soong and Hanson [14], shear-based actuators were proposed only recently by Sun and Zhang [15, 21], through a preliminary study with a commercial finite-element (FE) analysis code [15] and a theoretical model [21]. Mechanical and FE models were also proposed by Benjeddou *et al* [4–6]. They used the stress-induced piezoelectric coupling constant e_{15} of an axially poled lead zirconate-titanate (PZT) layer or patch sandwiched between thin elastic layers. Detailed comparisons of their results to those in [15, 21] can be found in [5]. d_{15} -based torsional actuators were also proposed recently for the production of large angular displacement and torque [11]. Actuator designs and assembly methods, materials preparation, poling procedures, test results for joint strengths, and actuator output capabilities are discussed. The above report [11] pointed out that current

commercially available PZT piezoceramics are optimized for their extension piezoelectric response but not for their shear properties.

A sandwich beam finite element capable of treating both shear and extension actuation mechanisms was presented and validated by the present authors in [5]. Based on this recently proposed unified FE approach, this paper discusses both *extension* and *shear actuation mechanisms* theoretically and numerically, with special emphasis on the comparison of static actuation performance of such mechanisms. Segmented adaptive cantilever beams are investigated for this purpose. *Extension actuation mechanism* is studied by letting the beam surface layers active with transverse polarization, whereas *shear actuation mechanism* is studied by activating the piezoelectric core poled axially. For each case study, static deflections and stresses, and vibration characteristics are compared for several parameter variations, namely, structure/actuator stiffness and thickness ratios, actuator position and length. To the authors' knowledge, this is the first detailed theoretical and numerical comparative study of the actuation performance and parametric analysis of these basic actuation mechanisms.

2. Theoretical analysis

Consider a sandwich beam made of either piezoelectric surface layers and elastic core, or piezoelectric core and elastic surface layers. To do so, each layer is considered piezoelectric but poled transversely for the surface layers and axially for the core. For both configurations, a transverse electric field is applied to the piezoelectric layer. To simulate elastic material, piezoelectric constants are set to vanish

(insulated layer). All layers are assumed perfectly bonded and in plane deformation state. Moreover, the transverse stress component is neglected compared to other components, and the transverse deflection is considered to be constant in the beam thickness. Sandwich beam surface layers are supposed to behave as Bernoulli–Euler beams while the core is assumed to be a Timoshenko beam. A local frame is attached to each layer at its left-end center, whereas the global frame is located at the left-end center of the beam, so that beam centroidal and elastic axes coincide with the x -axis. The length, width and thickness of the beam are denoted by L , b and h , respectively. The indices a , b , c indicate the top, bottom and core layer quantities and f index is used for surface layer parameters.

2.1. Displacement field equations

Starting with linear longitudinal displacements for each layer, and enforcing the interface displacement continuity conditions, axial displacement for the i th layer can be written in the form,

$$\begin{aligned} u_\alpha &= \bar{u}_\alpha + (z - z_\alpha)\beta & \bar{u}_\alpha &= \bar{u} \pm \frac{\tilde{u}}{2} \pm \frac{h_\alpha}{2}\beta \\ \beta &= -w' & \alpha &= a, b \\ u_c &= \bar{u}_c + z\beta_c. \end{aligned} \quad (1)$$

The prime denotes the first derivative in x , '+' for $\alpha = a$, '-' for $\alpha = b$. z_α defines the position of the elastic axes of the layer α in the global z -axis. \bar{u} and \tilde{u} are mean and relative axial displacements of upper and lower core skins, i.e.,

$$\bar{u} = \bar{u}_c = \frac{u^+ + u^-}{2} \quad \tilde{u} = h_c\beta_c = u^+ - u^- \quad (2)$$

where \bar{u}_c , β_c , h_c , u^+ and u^- are, respectively, mean displacement, bending rotation, core thickness and axial displacements of upper and lower core skins.

2.2. Reduced piezoelectric constitutive equations

A linear orthotropic piezoelectric material with symmetry axes parallel to the beam axes is considered here. c_{ij} , e_{kj} and ϵ_{kk} ($i, j = 1, \dots, 6; k = 1, 2, 3$) denote its elastic, piezoelectric and dielectric material constants.

For *extension actuation mechanism*, the piezoelectric beam surface layers are poled transversely and only the transverse electric field is important. Hence, three-dimensional linear constitutive equations of an orthotropic piezoelectric surface layer can be reduced [5] to

$$\begin{Bmatrix} \sigma_1 \\ D_3 \end{Bmatrix} = \begin{bmatrix} c_{33}^* & -e_{31}^* \\ e_{31}^* & \epsilon_{33}^* \end{bmatrix} \begin{Bmatrix} \varepsilon_1 \\ E_3 \end{Bmatrix} \quad (3)$$

where,

$$c_{11}^* = c_{11} - \frac{c_{13}^2}{c_{33}} \quad e_{31}^* = e_{31} - \frac{c_{13}}{c_{33}}e_{33} \quad \epsilon_{33}^* = \epsilon_{33} + \frac{e_{33}^2}{c_{33}}$$

and σ_1 , ε_1 , D_3 and E_3 are axial stress and strain, and transverse electric displacement and field. The modification of the material constants is due to the plane stress assumption

($\sigma_3 = 0$). Notice that the electromechanical coupling is between axial strain and transverse electric field only. This is the basic foundation of the extension actuation mechanism.

For the *shear actuation mechanism*, the piezoelectric core layer is poled in the axial direction. Its constitutive equations can be obtained from those of the surface layers, through a 90° rotation around out of plane direction followed by a 180° rotation around the transverse direction, so that axial and transverse indices interchange. Therefore, three-dimensional linear constitutive equations of the orthotropic piezoelectric core are [5]

$$\begin{Bmatrix} \sigma_1 \\ \sigma_5 \\ D_3 \end{Bmatrix} = \begin{bmatrix} c_{33}^* & 0 & 0 \\ 0 & c_{55} & -e_{15} \\ 0 & e_{15} & \epsilon_{11} \end{bmatrix} \begin{Bmatrix} \varepsilon_1 \\ \varepsilon_5 \\ E_3 \end{Bmatrix} \quad c_{33}^* = c_{33} - \frac{c_{13}^2}{c_{11}} \quad (4)$$

where σ_5 and ε_5 are transverse shear stress and strain. This modification is also due to the plane stress assumption for the core ($\sigma_3 = 0$). Notice that the electromechanical coupling is between shear strain and transverse electric field only. This is the origin of the newly defined concept of *shear actuation mechanism*.

2.3. Electric potential forms

This section defines electric potential equations for each actuation mechanism using strain-displacement relations, computed from the displacement field (1), and the electric field obtained from the reduced constitutive equations (3), (4) and substituted in the electrostatic equilibrium equation under free volumic charge density assumption.

For the *extension actuation mechanism*, integration of the following electrostatic equilibrium equation for the i th surface layer,

$$D_{\alpha 3,3} = 0 \quad (5)$$

leads to a quadratic electric potential in the surface layers,

$$\varphi_\alpha = \bar{\varphi}_\alpha + (z - z_\alpha)\frac{\tilde{\varphi}_\alpha}{h_\alpha} + \left(1 - \frac{4(z - z_\alpha)^2}{h_\alpha^2}\right)\frac{h_\alpha^2}{8}\frac{e_{31}^{\alpha*}}{\epsilon_{33}^{\alpha*}}w'' \quad (6)$$

where,

$$\tilde{\varphi}_\alpha = \varphi_\alpha^+ - \varphi_\alpha^- \quad \bar{\varphi}_\alpha = \frac{\varphi_\alpha^+ + \varphi_\alpha^-}{2}$$

φ_α^+ and φ_α^- are given electric potentials on upper and lower skins of the i th surface layer. Notice that the electric potential is the sum of a linear part, known from the given potentials φ_α^\pm , and a quadratic part, proportional to the beam curvature. The latter represents the induced potential, often neglected in the literature [2, 13].

For *shear actuation mechanism*, $D_{c1,1}$ is neglected compared to $D_{c3,3}$, hence equation (5) still holds and its integration provides a linear potential in the core,

$$\varphi_c = \bar{\varphi}_c + z\frac{\tilde{\varphi}_c}{h_c} \quad (7)$$

where $\bar{\varphi}_c$ and $\tilde{\varphi}_c$ are now mean and relative potentials of the core.

2.4. Variational formulation of the actuation problem

For the actuation problem, $\tilde{\varphi}$ are known (imposed), hence their virtual variations $\delta\tilde{\varphi}_i$ vanish, and the variational actuation problem can be written [4, 5] as

$$\delta H_m - \delta T = \delta W + \delta H_{me} \quad (8)$$

δT and δW are virtual variations of the kinetic energy and work done by external forces. They are similar for both mechanisms and were detailed in [5], but not repeated here. However, δH_m and δH_{me} are mechanical and mechanical–electric coupling contributions in the total virtual variation of the electromechanical energy δH .

2.4.1. Extension actuation mechanism. For identical surface layers, δH_m can be written as,

$$\delta H_m = \delta H_{cm} + \delta \tilde{H}_{fm} \quad (9)$$

where,

$$\delta H_{cm} = \int_0^L \left[c_{33}^{c*} A_c \tilde{u}' \delta \tilde{u}' + c_{33}^{c*} \frac{I_c}{h_c^2} \tilde{u}' \delta \tilde{u}' + c_{55}^c \frac{A_c}{h_c} \left(\frac{\tilde{u}}{h_c} + w' \right) \delta \tilde{u} + c_{55}^c A_c \left(\frac{\tilde{u}}{h_c} + w' \right) \delta w' \right] dx \quad (10)$$

$$\delta \tilde{H}_{fm} = \int_0^L \left\{ 2c_{11}^{f*} A_f \tilde{u}' \delta \tilde{u}' + \frac{1}{2} c_{11}^{f*} A_f (\tilde{u}' - h_f w'') \delta \tilde{u}' - \frac{1}{2} \left[c_{11}^{f*} A_f h_f \tilde{u}' - (c_{11}^{f*} A_f h_f^2 + 4\tilde{c}_{11}^f I_f) w'' \right] \delta w' \right\} dx \quad (11)$$

and

$$\tilde{c}_{11}^f = c_{11}^{f*} + \frac{(e_{31}^{f*})^2}{\epsilon_{33}^{f*}} \quad (12)$$

I_i and A_i are moment area, and area of the i th layer. Notice that the induced potential present in (6) has a passive effect on the surface layers through augmentation of their bending stiffness (12).

For active surface layers, the induced electric work δH_{me} is only due to the imposed potentials on the surface layers and can be seen as an ‘initial’ stress vector,

$$\delta H_{fme} = - \int_0^L \left[e_{31}^{f*} \frac{A_f}{h_f} (\tilde{\varphi}_a + \tilde{\varphi}_b) \delta \tilde{u}' + \frac{1}{2} e_{31}^{f*} \frac{A_f}{h_f} (\tilde{\varphi}_a - \tilde{\varphi}_b) \delta \tilde{u}' - \frac{1}{2} e_{31}^{f*} A_f (\tilde{\varphi}_a - \tilde{\varphi}_b) \delta w'' \right] dx. \quad (13)$$

Two particular cases could be distinguished, depending on the imposed potentials.

(a) $\tilde{\varphi}_a = \tilde{\varphi}_b = \tilde{\varphi}_f$, δH_{fme} reduces to

$$\delta \tilde{H}_{fme} = - \int_0^L 2e_{31}^{f*} A_f \frac{\tilde{\varphi}_f}{h_f} \delta \tilde{u}' dx. \quad (14)$$

For homogeneous material properties in axial direction and uniform applied potentials, (14) reduces to

$$\delta \tilde{H}_{fme} = -2e_{31}^{f*} A_f \frac{\tilde{\varphi}_f}{h_f} \delta \tilde{u} \Big|_0^L. \quad (15)$$

In this form, $\delta \tilde{H}_{fme}$ is interpreted as virtual work of boundary tractions $2e_{31}^{f*} A_f \tilde{\varphi}_f / h_f$ induced by the applied potentials. \tilde{u} is here the dual displacement parameter. Axial mean strain is then induced in this case.

(b) $\tilde{\varphi}_a = -\tilde{\varphi}_b = \tilde{\varphi}_f$, here, δH_{fme} reduces to

$$\delta \tilde{H}_{fme} = - \int_0^L e_{31}^{f*} A_f \tilde{\varphi}_f \left(\frac{\delta \tilde{u}'}{h_f} - \delta w'' \right) dx \quad (16)$$

For homogeneous material properties in the axial direction and uniform applied potentials, (16) becomes

$$\delta \tilde{H}_{fme} = -e_{31}^{f*} A_f \tilde{\varphi}_f \left(\frac{\delta \tilde{u}}{h_f} - \delta w' \right) \Big|_0^L. \quad (17)$$

Now, $\delta \tilde{H}_{fme}$ can be interpreted as virtual work of boundary tractions $e_{31}^{f*} A_f \tilde{\varphi}_f / h_f$ and moments $e_{31}^{f*} A_f \tilde{\varphi}_f$ induced by the applied potentials. \tilde{u} and $-w'$ are the dual relative displacement and bending rotation. The relative membrane strain and mean curvature are induced here. The first term of (17) can also be seen as virtual shear work of the interface shear forces $e_{31}^{f*} A_f \tilde{\varphi}_f / h_f$.

Using equations (8)–(13), the *extension actuation* problem takes the form

$$\delta \tilde{H}_{fm} + \delta H_{cm} - \delta T = \delta W + \delta H_{fme}. \quad (18)$$

From this, it can be concluded that piezoelectric material has a passive effect through the augmentation (12) of the bending stiffness due to the induced potential (quadratic term in (6)), and an active effect through an induced electric work (13). The latter can be due to boundary induced point tractions (15) or moments (17).

2.4.2. Shear actuation mechanism. Here, identical surface layers are not piezoelectric. Hence, equation (9) holds, but with $\tilde{c}_{11}^f = c_{11}^{f*}$. However, the induced electric work, seen as an initial stress work becomes

$$\delta \tilde{H}_{cme} = - \int_0^L e_{15}^c A_c \frac{\tilde{\varphi}_c}{h_c} \left(\frac{\delta \tilde{u}}{h_c} + \delta w' \right) dx. \quad (19)$$

Therefore, δH_{cme} can be interpreted as virtual work of distributed shear moments $e_{15}^c A_c \tilde{\varphi}_c / h_c$ induced by the applied electric potentials. Dual parameters are relative displacement \tilde{u} and bending rotations $-w'$. The first term of (19) can also be seen as virtual work of interface shear forces $e_{15}^c A_c \tilde{\varphi}_c / h_c^2$, where the dual displacement variable should be the relative displacement \tilde{u} .

Using equations (8), (9) and (19), the *shear actuation* variational equation is

$$\delta H_{fm} + \delta H_{cm} - \delta T = \delta W + \delta \tilde{H}_{cme}. \quad (20)$$

Since there is no induced potential in this case, the piezoelectric effect induces an equivalent electric work only. It is worthwhile to emphasize that, for the bending problem, the *shear actuation mechanism* induces *distributed shear moments* (19) whereas the *extension actuation mechanism* induces *boundary point moments* (17). Note also that there is no equivalent equation to the membrane problem using (15). Hence, the *shear actuation mechanism* is not useful for membrane problems.

3. FE discretization

Since \bar{u} and \tilde{u} are C^0 -continuous and w is C^1 -continuous, they are interpolated by Lagrange linear and Hermite cubic shape functions, respectively. Only electric potentials are imposed here, i.e. $\delta W = 0$. A classical FE procedure is followed to discretize the variational actuation problem (8) which leads to the following linear system for each actuation mechanism:

$$M\ddot{q} + (K_f + K_c)q = F_e \quad (21)$$

where $q = [\bar{u}_1, \tilde{u}_1, w_1, w'_1, \bar{u}_2, \tilde{u}_2, w_2, w'_2]^T$ is the degrees of freedom (dof) vector. M is the mass matrix of the sandwich beam. Its expression was given in [4, 5]. K_f , K_c and F_e are the surface layers and core stiffness matrices, and induced electric force/moment vector. Their expressions are now detailed for each actuation mechanism.

3.1. Extension actuation mechanism

The stiffness matrix of the piezoelectric surface layers has the expression

$$\bar{K}_f = 2 \int_0^L (c_{11}^{f*} A_f B_{fm}^T B_{fm} + \bar{c}_{11}^f I_f B_{fb}^T B_{fb}) dx \quad (22)$$

where, T states for transpose operation and B_{fj} ($j = m, b$) are membrane and bending deformation matrices. The stiffness matrix of the passive core is,

$$K_c = \int_0^L (c_{33}^{c*} A_c B_{cm}^T B_{cm} + c_{33}^{c*} I_c B_{cb}^T B_{cb} + c_{55}^c A_c B_{cs}^T B_{cs}) dx \quad (23)$$

where B_{cs} is the shear deformation matrix of the core. The electric force vector is, for $\tilde{\varphi}_a = \tilde{\varphi}_b = \tilde{\varphi}_f$

$$\bar{F}_{fe} = -2 \int_0^L e_{31}^{f*} A_f \frac{\tilde{\varphi}_f}{h_f} N'_i dx \quad (24)$$

and

$$\tilde{F}_{fe} = - \int_0^L e_{31}^{f*} A_f \tilde{\varphi}_f \left(\frac{1}{h_f} N'_i - N'_{w'} \right) dx \quad (25)$$

when $\tilde{\varphi}_a = -\tilde{\varphi}_b = \tilde{\varphi}_f$. N'_i ($i = \bar{u}, \tilde{u}, w'$) are the interpolation matrices derivatives of \bar{u} , \tilde{u} and w' .

The linear system (21) becomes, for a membrane actuation problem,

$$M\ddot{q} + (\bar{K}_f + K_c)q = \bar{F}_{fe} \quad (26)$$

and

$$M\ddot{q} + (\bar{K}_f + K_c)q = \tilde{F}_{fe} \quad (27)$$

for a bending problem.

It is worth noticing that when the induced potential is also neglected in the surface layers, there is no passive effect of the piezoelectric material; only an extra electric force vector is induced. Hence, the left-hand side of (26) and (27) are identical, but the piezoelectric material stiffness and mass are taken into account.

3.2. Shear actuation mechanism

In this case the bending actuation problem can be written as,

$$M\ddot{q} + (K_f + K_c)q = \tilde{F}_{ce} \quad (28)$$

where the stiffness matrix K_f is given by (22) but with c_{11}^{f*} instead of \bar{c}_{11}^f since the surface layers are passive here. The induced electric force vector is given by

$$\tilde{F}_{ce} = - \int_0^L e_{15}^c A_c \frac{\tilde{\varphi}_c}{h_c} B_{cs}^T dx. \quad (29)$$

This expression is the discretization of (19) since the shear strain is $\varepsilon_{cs} = (\tilde{u}/h_c) + w'$. A new interpretation of \tilde{F}_{ce} is obtained here. The induced electric work vector is only due to the thickness shear of the piezoelectric core.

4. Numerical comparisons

A sandwich beam finite element capable of treating both *shear* and *extension actuation mechanisms*, was implemented. It was validated in [4, 5]. Here, the emphasis is put on static and dynamic comparisons of both mechanisms. For the *extension actuation mechanism*, the top and bottom layers are supposed to be PZT5H piezoelectric material and the central core to be aluminum. The materials properties were given in [5]. For the *shear actuation mechanism*, top and bottom layers are assumed to be aluminum and the central core to be composed of a small patch of PZT5H piezoelectric material and, covering the rest of the core, a rigid foam material. The rigid foam has a density of 32 kg m^{-3} , a Young's modulus of 35.3 MPa and a shear modulus of 12.76 MPa .

4.1. Static analysis

The geometric configurations of both actuation mechanisms are presented in figure 1. Beams are clamped at $x = 0$ and free at $x = L$. Geometrical parameters, according to figure 1, are $L = 100 \text{ mm}$, $h = 16 \text{ mm}$ and $t = 1 \text{ mm}$. In order to bend the beam, voltages are applied at the top and bottom surfaces of piezoelectric layers, inducing bending electric forces. For the *shear actuation mechanism*, the voltage applied to the piezoelectric core has a value of $\tilde{\varphi}_c = -20 \text{ V}$, and for the *extension actuation mechanism*, voltages applied to surface actuators are $\tilde{\varphi}_f = -10 \text{ V}$.

Different arguments were used to compare both actuation mechanisms. First of all, a numerical analysis of the influence of actuator position and length in beam tip displacement is presented. Then, the longitudinal stress and shear strain in the core layer induced by the beam deflection are evaluated for both actuation mechanisms. Finally, variations of beam tip displacement with structure/actuator stiffness and thickness ratios are considered.

For the first analysis, the actuator's position and length vary in the range $15\text{--}60 \text{ mm}$ and $5\text{--}15 \text{ mm}$, respectively. In each case, the beam tip displacement induced by the applied electric forces is evaluated. Figure 2 shows the effect of actuator position and length in beam tip deflection for both actuation mechanisms. It is clear that *extension actuation*

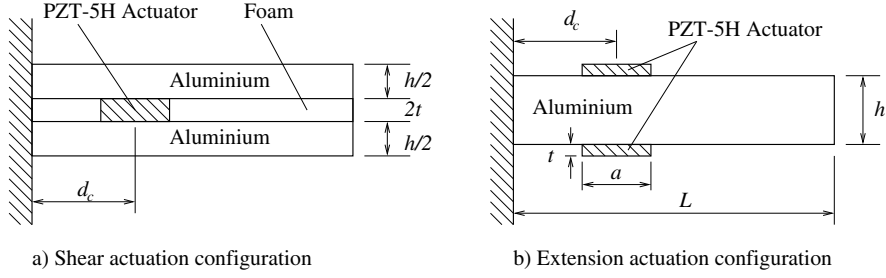


Figure 1. Cantilever sandwich beam, shear (a) and extension (b) actuation configurations.

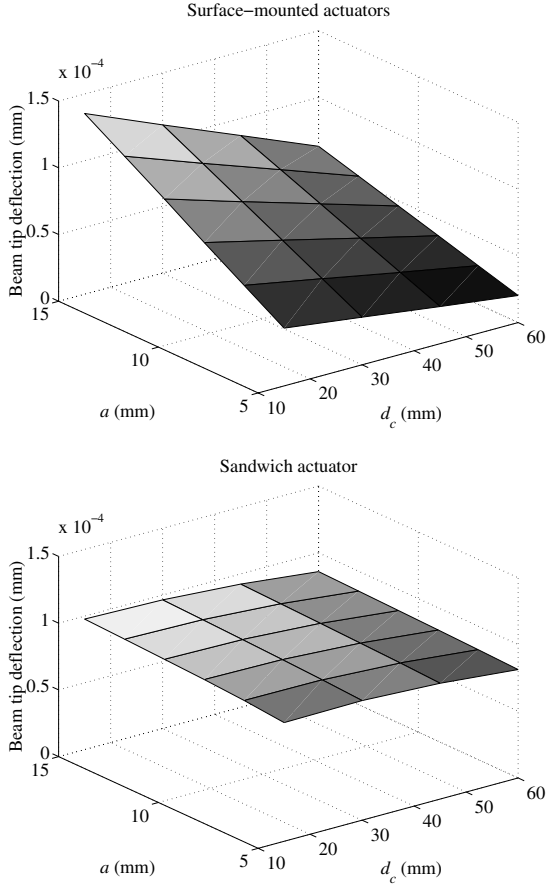


Figure 2. Variation of beam tip deflection with actuator position d_c and length a .

mechanism is strongly dependent on position and length of the actuator, whereas *shear actuation mechanism* has almost the same effectiveness in all the range. Figure 2 also confirms that surface-mounted actuators are only efficient when they are long and near the clamped end. In contrast, shear actuators can retain their efficiency even with very short lengths and in a quite large position range.

Furthermore, as can be seen in figure 3, the longitudinal stress in the piezoelectric actuator is much lower for *shear actuation mechanism* than for the *extension mechanism*. However, the induced longitudinal stress in the structure is almost the same for both mechanisms. It is worth noticing also that the axial stresses in the structure and in the actuator are of the same order for the *shear actuation mechanism*, whereas for the *extension*, stresses in the actuator are

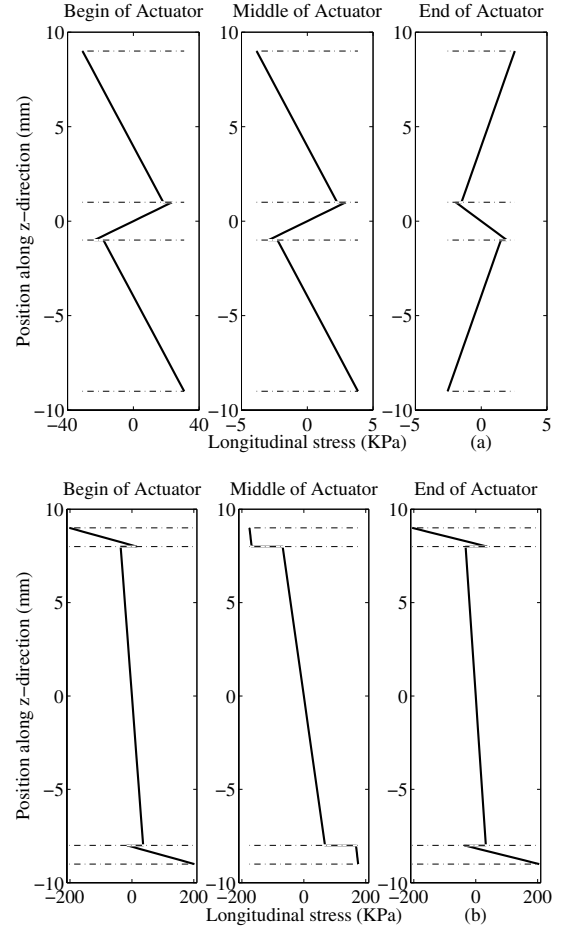


Figure 3. Longitudinal stress along the z -direction for shear (a) and extension (b) actuation mechanisms.

approximately ten times larger than those in the structure. Figure 4 presents shear strains in the core layer for both mechanisms. It shows the shear strain induced by the piezoelectric shear actuator (figure 4(a)) and confirms the theoretical prediction that out-of-phase extension actuators induce only pure bending (figure 4(b)).

As piezoelectric actuation is applied, in practice, to different kinds of structures, it is worthwhile to investigate the effect of structure stiffness in the effectiveness of the actuator. Therefore, an analysis of this effect was achieved by the evaluation of the beam tip displacement through piezoelectric actuation for several structure stiffness ratios. These are defined as c_{11}^*/c_{33}^* for the shear actuation mechanism and

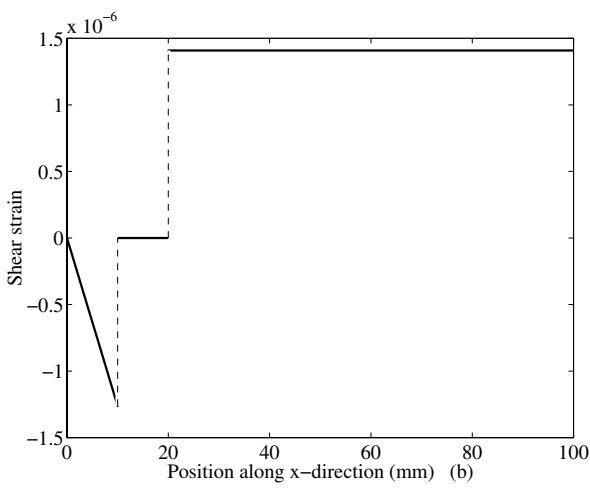
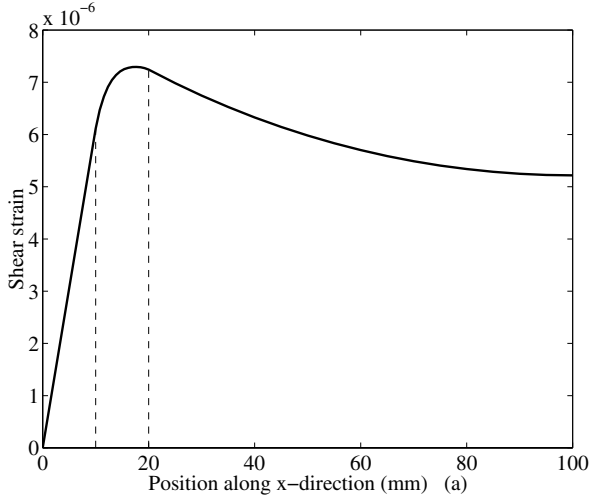


Figure 4. Shear strain in the core along the x -direction for shear (a) and extension (b) actuation mechanisms.

c_{33}^*/c_{11}^* for the extension actuation mechanism. As can be seen in figure 5, surface-mounted actuators are more efficient when their stiffness is greater than that of the structure. Nevertheless, although sandwich actuators are not so efficient in all of the range, especially in the most common structure/actuator stiffness ratio range between one and 10. This is a great advantage for the shear actuation mechanism since, in contrast to the extension mechanism, its performance is preserved for stiffer structures. Figure 5 shows also that there is an optimal stiffness ratio range for which the shear actuation mechanism is always better than the extension mechanism. This is the case for PZT5H case and a stiffer elastic material in the faces.

The variation of the beam tip deflection with the actuator thickness was also evaluated. It can be seen in figure 6 that the shear actuation mechanism performs better than the extension mechanism for thicker actuators, as can be expected. Also, for the case presented, the shear actuation mechanism is more efficient in a medium range $t = 0.5\text{--}5$ mm, whereas the extension actuation mechanism is more efficient in a low range ($t < 1$ mm). It can also be noticed from figure 6 that for $t > 1$ mm, the shear actuation mechanism is always more efficient than the extension mechanism.

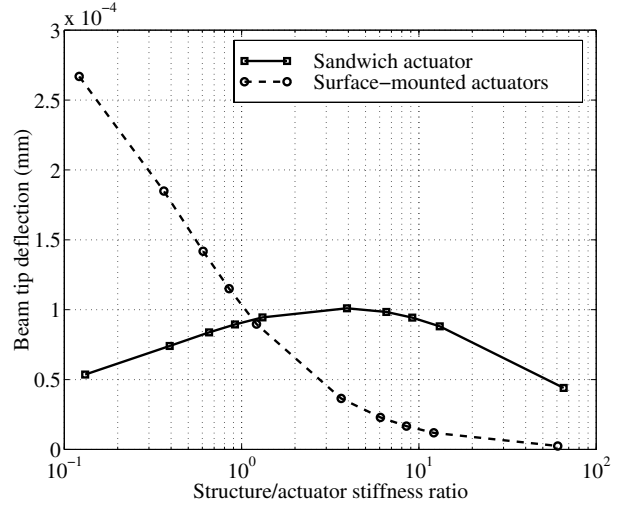


Figure 5. The variation of beam tip deflection with the structure/actuator stiffness ratio.

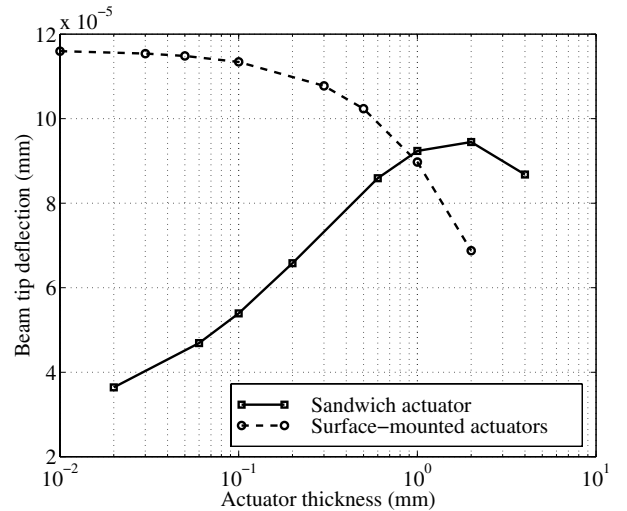


Figure 6. The variation of beam tip deflection with actuator thickness.

4.2. Dynamic analysis

Natural modes and frequencies were evaluated for both *shear* and *extension actuation mechanisms*. Material data are the same as presented in [12] and the geometric representation of the beam is presented in figure 1(b) where $L = 50$ mm, $h = 2$ mm, $t = 0.5$ mm, $d_c = 11$ mm and $a = 20$ mm. The equivalent shear actuation beam is represented by figure 1(a). Since an evaluation of eigenfrequencies for the shear actuation mechanism was not found in the literature, only the extension actuation mechanism numerical eigenfrequencies were compared to analytical [12] eigenfrequencies. Equivalent natural frequencies were, then, evaluated for the shear actuation mechanism.

From table 1 it is clear that the FE results for the natural bending frequencies showed good agreement with analytical results. A graphical representation of the first three bending modes is shown in figure 7. It can be seen that in all three bending modes, the actuator deformation is lower for the shear actuation mechanism.

Table 1. First five natural bending frequencies (Hz) for a shear and extension actuated cantilever beam.

		1	2	3	4	5
Shear actuation	Present FE results	989	3916	8374	17416	26025
	Analytical results [12]	1084	4430	12422	23499	38014
Extension actuation	Present FE results	1030	4230	12000	23500	38500
	Error (%)	5.24	4.73	3.52	-0.00	-1.26

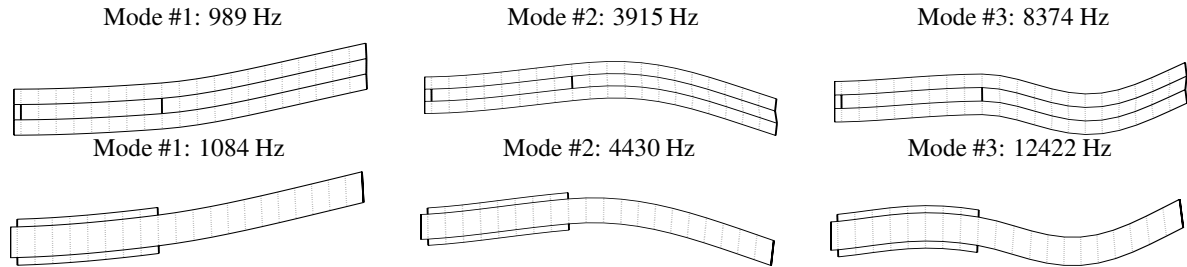


Figure 7. The natural bending modes and frequencies for shear and extension actuation mechanisms.

5. Conclusions

Theoretical and numerical comparisons of shear and extension actuation mechanisms for statics and dynamics of smart beams were presented. It was shown that surface-mounted actuators, acting through the e_{31} piezoelectric constant, induce boundary concentrated forces and moments in the structure. Whereas, sandwich shear actuators, acting through the e_{15} piezoelectric constant, induce distributed moments in the structure. Therefore, less debonding and singularity problems are expected for shear actuators.

Comparisons between both actuation mechanisms in static piezoelectric actuation were analyzed for several parameter variations, such as actuator location and length and structure/actuator stiffness and thickness ratios. It was found that extension actuators are efficient when they are long and placed near the clamped end of the beam. Shear actuators, however, retain their effectiveness, even for very short lengths, over a larger range of positions. Longitudinal stress evaluation showed advantages for the shear actuation mechanism, since levels of stress in the actuator are smaller. Also, longitudinal stress discontinuities at layer interfaces are smaller, leading to the best protection against interface debonding problems. It was also shown that shear actuator performance is less dependent of structure stiffness. Moreover, for stiffer structures, the shear actuation mechanism performs better than extension mechanism. It was also found that only thin extension actuators are efficient; shear actuators are more effective for a medium thickness range.

Dynamic analysis of both actuation mechanisms was presented, through the evaluation of natural bending frequencies and modes. The numerical results showed good agreement with the analytical results. The vibration modes are equivalent in both mechanisms; nevertheless shear actuators are less deformed than extension actuators.

The present work has been extended to active [19] and hybrid active-passive [18] control applications. Therefore, a new adaptive sandwich beam element [6] based on a different kinematic description is used. It takes into account the extra shear (due to the sliding of the faces against the core) in

order to better represent the energy dissipation mechanism of hybrid active-passive damping treatments.

References

- [1] Baz A 1997 Boundary control of beams using active constrained layer damping *J. Vib. Acoust.* **119** 166–72
- [2] Benjeddou A 2000 Advances in piezoelectric finite elements modeling of adaptive structural elements: a survey *Comput. Struct.* **74** 465–76
- [3] Benjeddou A 1999 Recent advances in hybrid active-passive vibration control *J. Vib. Control* submitted
- [4] Benjeddou A, Trindade M A and Ohayon R 1997 A finite element model for shear actuated adaptive structures *8th Int. Conf. Adaptive Structure Technology* (Lancaster, PA: Technomic) pp 133–42
- [5] Benjeddou A, Trindade M A and Ohayon R 1997 A unified beam finite element model for extension and shear piezoelectric actuation mechanisms *J. Intell. Mater. Syst. Struct.* **8** 1012–25
- [6] Benjeddou A, Trindade M A and Ohayon R 1999 New shear actuated smart structure beam finite element *AIAA J.* **37** 378–83
- [7] Chee C Y K, Tong L and Steven G P 1998 A review on the modelling of piezoelectric sensors and actuators incorporated in intelligent structures *J. Intell. Mater. Syst. Struct.* **9** 3–19
- [8] Crawley E F and Anderson E H 1990 Detailed models of piezoceramic actuation beams *J. Intell. Mater. Syst. Struct.* **1** 4–25
- [9] Hagood N, Kindel R, Ghandi K and Gaudenzi P 1993 Improving transverse actuation of piezoceramics using interdigitated surface electrodes *North American Conf. on Smart Structures and Materials* vol 1917 (Bellingham, WA: SPIE) pp 341–52
- [10] Huang S C, Inman D J and Austin E M 1996 Some design considerations for active and passive constrained layer damping treatments *Smart Mater. Struct.* **5** 301–13
- [11] Kim G *et al* 1997 Composite piezoelectric assemblies for torsional actuators *Naval Research Laboratory and PSU Report NRL/MR/6380-97-7997*
- [12] Lin M W, Abatan A O and Rogers C A 1994 Application of commercial finite element codes for the analysis of induced strain-actuated structures *2nd Int. Conf. Intelligent Materials* (Lancaster, PA: Technomic) pp 846–55

- [13] Rahmoune M, Osmont D, Benjeddou A and Ohayon R 1996 Finite element modeling of a smart structure plate system *7th Int. Conf. Adaptive Structures Technology* (Lancaster, PA: Technomic) pp 463–73
- [14] Soong T T and Hanson R D 1993 Recent development in active and hybrid control research in the US *Int. Workshop on Structure Control* CE-9311 (USC) pp 483–90
- [15] Sun C T and Zhang X D 1995 Use of thickness shear mode in adaptive sandwich structures *Smart Mater. Struct.* **4** 202–6
- [16] Sunar M and Rao S S 1999 Recent advances in sensing and control of flexible structures via piezoelectric materials technology *Appl. Mech. Rev.* **52** 1–16
- [17] Tomlinson G R 1996 An overview of active/passive damping techniques employing viscoelastic materials *3rd Int. Conf. on Intell. Mater. and 3rd Eur. Conf. on Smart Structures and Materials* **2779** (Bellingham, WA: SPIE) pp 656–69
- [18] Trindade M A, Benjeddou A and Ohayon R 1999 Modeling of frequency-dependent viscoelastic materials for active–passive vibration damping *J. Vib. Acoust.* at press
- [19] Trindade M A, Benjeddou A and Ohayon R 1998 Parametric analysis of the vibration control of sandwich beams through shear-based piezoelectric actuation *J. Intell. Mater. Syst. Struct.* submitted
- [20] Varadan V, Lim Y-H and Varadan V 1996 Closed loop finite-element modeling of active/passive damping in structural vibration control *Smart Mater. Struct.* **5** 685–94
- [21] Zhang X D and Sun C T 1996 Formulation of an adaptive sandwich beam *Smart Mater. Struct.* **5** 814–23